Influence of whey protein-xanthan gum stabilized emulsion on stability and *in vitro* digestibility of encapsulated astaxanthin

Nuntarat Boonlao, Smriti Shrestha, Muhammad Bilal Sadiq, Anil Kumar Anal

PII: S0260-8774(19)30502-3

DOI: https://doi.org/10.1016/j.jfoodeng.2019.109859

Reference: JFOE 109859

To appear in: *Journal of Food Engineering*

Received Date: 3 October 2019

Revised Date: 30 November 2019

Accepted Date: 1 December 2019

Please cite this article as: Boonlao, N., Shrestha, S., Sadiq, M.B., Anal, A.K., Influence of whey protein-xanthan gum stabilized emulsion on stability and *in vitro* digestibility of encapsulated astaxanthin, *Journal of Food Engineering* (2020), doi: https://doi.org/10.1016/j.jfoodeng.2019.109859.

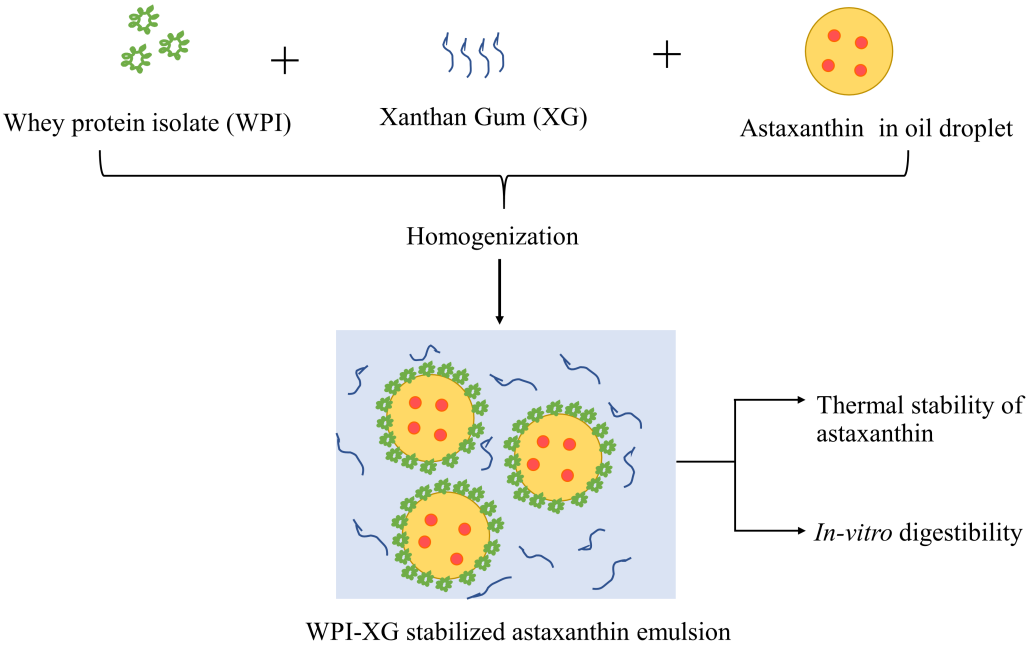

WPI-XG stabilized astaxanthin emulsion

Influence of whey protein-xanthan gum stabilized emulsion on stability and *in vitro* digestibility of encapsulated astaxanthin

Nuntarat Boonlao[1], Smriti Shrestha[1], Muhammad Bilal Sadiq[2], Anil Kumar Anal[1*]

[1]Food Engineering and Bioprocess Technology, Department of Food, Agriculture and Bioresources, Asian Institute of Technology, Pathum Thani, Thailand

[2]School of Life Sciences, Forman Christian College (A Chartered University), Lahore, 54600, Pakistan.

Corresponding author: Anil Kumar Anal, Department of Food Agriculture and Bioresources, Asian Institute of Technology, Pathum Thani 12120, Thailand

Email: anilkumar@ait.asia; anil.anal@gamil.com Tel: + 66 25246110, Fax: +66-2-5246200

Abstract

The combination of proteins and polysaccharides has potential to act as good emulsifiers and stabilizers. The aim of this study was to evaluate the stability of the emulsion system stabilized by whey protein isolate (WPI) (2-5 wt%) and xanthan gum (XG) (0.25 and 0.5 wt%). Furthermore, the influence of WPI-XG emulsion system on the thermal stability of incorporated astaxanthin under different storage temperatures (5, 25, 37, 55 and 70 ºC) and *in vitro* digestion were investigated. The emulsion system with higher XG concentration (0.5 wt%) exhibited the highest viscosity, emulsion stability, and creaming stability. The WPI-XG stabilized emulsion exhibited higher stability of astaxanthin at lower storage temperature (5, 25 and 37 ºC) with 10-12% astaxanthin loss during 15 days of storage. During *in vitro* digestion, emulsion stabilized by WPI-XG demonstrated influence on droplet digestion process, significantly ($p<0.05$) lower lipid digestibility and lower astaxanthin digestion (12.6%) in comparison to emulsion stabilized by WPI alone. This research study provides platform for designing fortified food or beverage systems incorporated with hydrophobic bioactive compounds for better stability and delivery to target sites.

Keywords: Whey protein isolate; xanthan gum; astaxanthin; emulsion; *in vitro* digestion

1. Introduction

Emulsion-based delivery system is an effective approach to improve the water solubility and bioavailability of hydrophobic bioactive compounds (Liu et al., 2016). Proteins and polysaccharides are the biopolymers commonly used as emulsifiers/stabilizers. Due to amphiphilic character, proteins can strongly adsorb at oil-water interface and provide electrostatic and/or steric repulsion force which prevents droplet aggregation and coalescence (Jain and Anal, 2018). On the other hand, polysaccharides increase the viscosity of aqueous phase and enhance the stability of emulsion by inhibiting the droplets movement, and hence are used as stabilizer/thickening agents (Ozturk and McClements, 2016).

The interaction between proteins and polysaccharides is a natural phenomenon of great importance in food systems for stabilization of colloidal systems, particularly emulsion-based delivery systems (Anal et al., 2019). The combination of proteins and polysaccharides under appropriate conditions (concentration, protein-to-polysaccharide ratio, pH, ionic strength, temperature) exhibits a great improvement in emulsion stability (Donald, 2008; Guzey and McClements, 2006). These biopolymeric interactions, therefore, combine the stabilizing effect of polysaccharide with the emulsifying ability of protein in the formulation of stable colloidal food formulations. The mechanism of emulsion stabilization is based on polysaccharide absorption ability and interaction with the proteins. Firstly, protein-polysaccharide complex is formed due to polysaccharides adsorption to the surface of protein-coated droplet via the electrostatic interactions between proteins and polysaccharides (Qiu et al., 2015a). Secondly, proteins and polysaccharides can stabilize

emulsion without developing any attractive interactions, for instance, proteins adsorb at oil-water interface, while polysaccharides only modify the viscosity of aqueous phase due to their non-adsorbing nature (Bouyer et al., 2012).

Xanthan gum (XG) is a high molecular weight (1.5×10^6 to 5×10^6 g/mol) anionic heteropolysaccharide produced by the microorganism *Xanthomonas campestris*. XG is a non-adsorbing polysaccharide which does not bind to protein-stabilized droplet surfaces. The addition of XG into oil-in-water emulsion improves the emulsion stability by increasing the viscosity of aqueous phase and restricting the mobility of oil droplets (Khouryieh et al., 2015; Moschakis et al., 2005). Bouyer et al. (2013), reported that β-lactoglobulin stabilized emulsion in the presence of XG exhibited the better efficacy in comparison to β-lactoglobulin alone and β-lactoglobulin-gum arabic stabilized emulsion. Park et al. (2018) investigated the effect of XG addition on lipolysis and β-carotene bioaccessibility of the rice starch-based filled hydrogel loaded with β-carotene. The highest rate and overall extent of lipid digestion was exhibited by the hydrogel in the presence of XG at the concentration of 1 and 2 wt%. Further, the bioaccessiblity of β-carotene was observed to decrease with the increase in XG concentration. It is, therefore, important to understand the effect of XG on the behavior of emulsion during passage through the gastrointestinal tract, which includes emulsion fate, lipid digestion and the bioaccessibility of encapsulated bioactive compounds.

Astaxanthin is a deep red color carotenoid synthesized as metabolic product by several microorganisms. Green algae *Haematococcus pluvialis*, is one of the main sources of natural astaxanthin (Feng et al., 2018; Martínez-Delgado et al., 2017). The consumption of astaxanthin presents a great deal of health benefits, such as prevention of oxidative stress and cardiovascular diseases (Martínez-Delgado et al., 2017), due to which it is gaining interest as a nutraceutical ingredient in the fortification of food products. However,

astaxanthin has poor water solubility, low bioavailability and prone to degrade by exposure to oxygen, heat and light (Taksima et al., 2015). Emulsion-based delivery systems have been used for improving solubility and bioavailability of astaxanthin (Meor Mohd Affandi et al., 2011; Ribeiro et al., 2005). Cod liver oil is a source of omega-3 fatty acids, especially eicosapentanoic acid (EPA) and docosahexaenoic acid (DHA) and vitamins A, D and E (Calvano et al., 2008). Therefore, the cod liver oil is used as an oil phase to develop the delivery system for lipophilic bioactive ingredients to fortify the food emulsions (Farvin et al., 2014).

To our knowledge, none of the study has reported the formulation of WPI-XG stabilized emulsion system to encapsulate astaxanthin oleoresins. The main purpose of this study was to investigate the effect of WPI-XG stabilized emulsion system on the thermal stability and *in vitro* digestion behavior of encapsulated astaxanthin oleoresin extracted from microalgae *Haematococcus pluvialis.*

2. Materials and methods

2.1 Materials

Haematococcus pluvialis astaxanthin oleoresin (10 wt% astaxanthin) was purchased from Yunnan Alphy Biotech Co. Ltd, China. Cod liver oil (Engelvaer Norwegian) was acquired from Piping Rock Health Products Co. Ltd, New York, USA. Whey protein isolate (WPI) was acquired from Club Protein Co. Ltd, Thailand. Xanthan gum (XG) was obtained from Union Chemical 1986 Co. Ltd, Thailand. All other chemicals/reagents used were analytical grade.

2.2 Preparation of wall materials

Mixture of WPI and XG at different proportions was used as wall material to formulate oil-in-water emulsion. Effects of varying XG concentrations (0, 0.25 and 0.5 wt%) and WPI concentrations (2, 3, 4 and 5 wt%) on the emulsion viscosity, emulsion stability and creaming index were studied. In each formulation, wall material (mixture of WPI and XG) was dispersed in distilled water and sodium azide (0.04 wt%) was added into the mixture to inhibit microbial growth (Chityala et al., 2016). The mixture was continuously stirred at 100 rpm (VelpScientifica, Europe) for at least 6 h to ensure hydration.

2.3 Preparation of astaxanthin-loaded emulsions

The astaxanthin-loaded oil-in-water emulsion was prepared by following (Liu et al., 2016) with slight modification. The oil phase was prepared by dispersing 1 g of astaxanthin oleoresin into 100 g of cod liver oil by magnetic stirring at 100 rpm for 2 h. The wall material solution was used as an aqueous phase. The oil phase was added into the wall material solution and total solid content of each emulsion system was adjusted to15% (w/w). Initially, coarse emulsions were prepared by blending the mixture through a high-speed blender (OTTO, BE-127/127A, Thailand) for 2 min at 2000 rpm. The coarse emulsions were then passed through a high-pressure homogenizer (IKA Labor-pilot, 2000/4, Staufen, Germany) for three passes at 500 bars to form an oil-in-water emulsion. The final emulsions were adjusted to pH 7 using 1 N HCl or 1 N NaOH. The emulsions were then kept in a sterilized test tubes and stored at 5 ± 1 ºC in dark conditions to prevent the degradation of astaxanthin by the effect of light (Tamjidi et al., 2014a).

2.4 Emulsion stability, creaming index, and viscosity

The emulsion stability was measured by following the method of Tamnak et al. (2016). The emulsion (10 mL) was centrifuged at 2000 × g for 5 min at 4 °C. The emulsion stability was calculated by using Eq. (1).

$$Emulsion\ stability\ (\%) = \frac{H_2}{H_1} \times 100 \quad (1)$$

Where H_1 is the initial height of fresh emulsion and H_2 is the height of emulsion after centrifugation.

The creaming index was determined by using Eq. (2). Emulsion (10 mL) was placed in glass test tube with cap and stored at 25 ± 1 ºC for 15 days. The height of the cream and serum layer was measured.

$$Creaming\ Index\ (\%) = \frac{Serum\ layer\ height}{Total\ height\ of\ emulsion} \times 100 \quad (2)$$

Emulsion viscosity was measured following the method described by Jain and Anal (2018). The viscosity of emulsions was determined using a Brookfield digital viscometer at 25 ºC (DV-II + Pro Viscometer, Brookfield Engineering Laboratories, Stoughton, USA). Viscosity was measured within 24 h of preparation and expressed in mPa.s.

The optimized emulsions with higher emulsion viscosity, emulsion stability and lower creaming index were selected for further characterization and classified as E1, E2, E3 and E4 emulsion systems with varying concentration of WPI (2, 3, 4 and 5 wt%, respectively) and fixed concentration of XG (0.5 wt%).

2.5 Particle size and particle charge measurement

The mean particle diameter (z-average), polydispersity index (PDI) and zeta potential of emulsions were determined by dynamic light scattering technique using Zetasizer Nano ZS (ZEN 3600, Malvern 220 Instrument Ltd., Malvern, Worcestershire, UK). Prior to analysis, emulsion samples were diluted (100 times) with distilled water to prevent multiple scattering effects. All the measurements were carried out at 25 ºC.

2.6 Microstructure

Microscopic images of emulsion samples were studied using light microscope (Olympus CX31, Tokyo, Japan) at 40× objective magnification. Freshly prepared emulsion sample (50 µL) was dropped on a clear glass slide with a coverslip and observed under microscope.

2.7 Effect of storage temperatures on thermal stability of the astaxanthin-loaded emulsion

Astaxanthin-loaded emulsions were stored in dark conditions at different temperatures (5 ± 1, 25 ± 1, 37 ± 1, 55 ± 1 and 70 ± 1 °C) for the period for 15 days. Emulsions were stored in cold storage room (5 ± 1 ºC), room temperature (25 ± 1 ºC) and hot air oven (37 ± 1, 55 ± 1 and 70 ± 1 °C) to maintain the different storage temperatures. The storage temperature was monitored by calibrated digital thermometer. Thermal stability of astaxanthin was evaluated in terms of change in color and astaxanthin concentration in emulsions during the storage period. The color measurement was performed by following the method reported by Davidov-Pardo et al. (2016) in the term of L^*, a^*, b^* color parameters of CIELAB system using a colorimeter (Hunter Lab Spectrocolorimeter, TC-P III A, Tokyo Denshoku Co., Ltd., Japan). The total color difference (ΔE) was calculated using following Eq. (3).

$$\Delta E = \sqrt{(L^* - L_i^*)^2 + (a^* - a_i^*)^2 + (b^* - b_i^*)^2} \quad (3)$$

Where L^*, a^*, b^* are color coordinates measured at specific time, and L_i^*, a_i^*, b_i^* are the initial values of color coordinates measured immediately after emulsion preparation.

The concentration of astaxanthin in the emulsion systems was determined by following the method of Khalid et al. (2017) with slight modifications. The emulsions (50 µL) were diluted in 4.95 mL of organic solvent (dichloromethane: methanol = 2:1, v/v) and then

centrifuged at 4472 × g for 20 min. Astaxanthin was measured from the supernatant using UV-VIS spectrophotometer (Shimadzu, Kyoto, Japan) at 480 nm. The emulsion without astaxanthin was used as a blank. A calibration curve was developed by dissolving the astaxanthin standard in the organic solvent (dichloromethane: methanol = 2:1, v/v) in a concentration range of 0 to 12 mg/L (r^2 = 0.986). The stability of astaxanthin in emulsion system was expressed as astaxanthin retention (%), which was calculated by following Eq. (4).

$$\text{Astaxanthin retention (\%)} = \frac{C}{C_0} \times 100 \quad (4)$$

Where C is the astaxanthin concentration at certain day and C_0 is the astaxanthin retention at 0 day

According to Niamnuy et al. (2008), astaxanthin degradation rate was calculated following fist-order kinetic model as shown in Eq. (5).

$$ln\left(\frac{C}{C_0}\right) = -kt \quad (5)$$

Where C_0 and C are astaxanthin concentrations (mg/mL) at time 0 and specific time t (day) respectively; t is the storage time (day); k is the temperature dependent rate constant (day^{-1}).

The degradation rate (temperature dependent) was measured by using the Arrhenius relationship (Eq. 6).

$$ln(k) = ln(A) - \frac{E_a}{RT} \quad (6)$$

where k is the astaxanthin degradation rate constant; A is a preexponential factor; E_a is the activation energy; R is the universal gas constant (8.3145 J mol^{-1} K^{-1}); T is the absolute temperature in Kelvin.

2.8 *In vitro* digestion of astaxanthin-loaded emulsion

The astaxanthin-loaded emulsions were passed through an *in vitro* digestion model including the simulated mouth, stomach, and small intestinal phases following the method as described by Shrestha et al. (2018) with slight modification.

Initial stage: The initial emulsion system was comprised of astaxanthin-loaded WPI-XG stabilized emulsion. The emulsion (10 mL) was transferred to a glass beaker and maintained at a temperature of 37 ºC in a water bath.

Simulated mouth phase: Simulated saliva fluid (SSF) was prepared by mixing 0.1594 g NaCl, 0.0202 g KCl, amylase (0.87% w/v) and 0.022 g mucin into phosphate buffer solution (PBS 10 mM, pH 7) to obtain final volume of 100 mL and the pH of SSF was adjusted to 6.8. SSF (5 mL) was mixed to the initial emulsion system (5 mL) and maintained at 37 ºC in a water bath for 5 min with continuous shaking at 100 rpm.

Simulated gastric phase: Simulated gastric fluid (SGF) was prepared by dissolving 0.32 wt% pepsin and 0.2 wt% NaCl in 10 mM phosphate buffer solution (pH 2.5). SGF (10 mL) was added to the resulted mixture from the simulated mouth phase (10 mL). The mixture was incubated at 37 ºC for 2 h with a continuous shaking at 100 rpm in the water bath.

Simulated intestinal phase: Simulated intestinal fluid (SIF) contained 39 mM K_2HPO_4, 150 mM NaCl and 30 mM $CaCl_2$.The resultant mixture from the gastric phase (20 mL) was mixed with SIF (20 mL) followed by the addition of bile salt extract (5 mg/mL) and pancreatin (1.6 mg/mL). The pH of the resulting mixture was adjusted at 7 and placed in a water bath at 37 ºC with continuous shaking for 2h.

Emulsion samples from each stage of the *in vitro* digestion process were collected and diluted (100 times) by respective buffer of each digestion phase (without enzymes). The

diluted emulsion samples were analyzed for mean particle diameter (z-average), and zeta potential by dynamic light scattering technique using Zetasizer Nano ZS.

2.9 Determination of free fatty acid released

The degree of lipid digestion was determined in term of free fatty acids (FFAs) released within small intestine using titration method (Pinsirodom and Parkin, 2001). The intestinal digesta (5 mL), acetone (10 mL) and 3 drops phenolphthalein (1%, w/v) were mixed together and titrated with 0.1 M NaOH. The volume of NaOH used to obtain the endpoint was recorded. The amount of free fatty acid released was calculated by using Eq. (7).

$$FFA\ (\%) = \left(\frac{V_{NaOH} \times m_{NaOH} \times MW_{oil}}{2 \times W_{oil}}\right) \times 100 \quad (7)$$

where V_{NaOH} is the volume of NaOH required for titration (mL); m_{NaOH} is the molarity of used NaOH; MW_{oil} is the molecular weight of oil (g mol^{-1}); W_{oil} is the initial weight of oil.

2.10 Determination of astaxanthin digestion

The digestion of astaxanthin after passing through *in vitro* digestion was measured by following the method as described by Salvia-Trujillo et al. (2013) with some modification. Raw digesta (10 mL) was centrifuged (EBA8S, Hettich, Germany) at 716 × g for 60 min at 25 ºC. After centrifugation, the supernatant containing astaxanthin solubilized in mix micelle was collected. A top layer of non-digested oil was discarded from the micelle fraction before analysis. The aliquots (5 mL) of raw digesta or micelle fraction were mixed with 5 mL organic solvent (dichloromethane: methanol = 2:1, v/v) and centrifuged at 137 × g for 10 min at 25 ºC. The bottom layer which solubilized astaxanthin was collected, whereas the top layer was mixed again with organic solvent (5 mL) and the same procedure was followed. The bottom part of organic solvent layer was mixed into the

previous one and the absorbance was measured at 480 nm using UV-VIS spectrophotometer (Shimadzu, Kyoto, Japan). The digestion of astaxanthin was calculated using Eq. (8).

$$Astaxanthin\ digestion\ (\%) = 100 \times \left(\frac{C_{Micelle}}{C_{Raw\ digesta}}\right) \quad (8)$$

Here $C_{Micelle}$ is the astaxanthin concentration in micelles fraction and $C_{Raw\ digesta}$ is the astaxanthin concentration in raw digesta

2.11 Statistical analysis

All experiments were performed in triplicates and the resulted were expressed as mean values with standard deviation. Statistical testing was carried out by using SPSS statistical software (SPSS, 22.0). Analysis of variance (ANOVA) and Tukey's HSD test were carried out to determine the significant differences ($p < 0.05$) among the mean observations.

3. Results and discussion

3.1 Effect of WPI and XG on the physical stability of astaxanthin-loaded emulsion

The effects of different concentrations of WPI and XG on viscosity, emulsion stability and creaming index of astaxanthin-loaded emulsions are summarized in Table1.

3.1.1 Viscosity

During 15 days of storage, the absence of XG, emulsions stabilized by WPI (2-4 wt%) alone had no significant effect on viscosity. Moreover, the emulsions stabilized by WPI alone exhibited the lowest viscosity indicating that presence of XG had significant role in the viscosity of emulsion (Chityala et al., 2016). At each WPI concentration (2-5 wt%), increase in XG concentration increased the viscosity of emulsions significantly ($p < 0.05$) which was due to the predominant thickening effect of XG. This result indicates that the

emulsion viscosity is proportional to the viscosity of the continuous phase (Khouryieh et al., 2015). Similarly, Sun et al. (2007) reported a sharp increase in an emulsion viscosity as XG concentration exceeded 0.2 wt%.

3.1.2 Emulsion stability

The emulsion stabilized by WPI-alone exhibited the lowest emulsion stability (6.67-7.22 %) whereas emulsions stabilized by WPI-XG mixture (with 0.5 wt% XG) exhibited the highest emulsion stability (94.39-99.02 %). At each WPI concentration, emulsion stability was increased with increase in XG concentration. Similarly, Xu et al. (2017) also reported an improvement in creaming stability of the emulsion at pH 7 stabilized by hydrolyzed rice glutelin in the presence of XG (0.4 wt%). However, in the absence of XG, WPI had no significant effect on emulsion stability. XG plays the role in emulsion stability due to following reasons: firstly, XG is a molecule with high molecular weight, charge density, and rigidity and thus it may adsorbed to positive patches on the surface of protein-coated droplets, leading to increases in the electrostatic and steric repulsive force between droplets (Protonotariou et al., 2013). Secondly, XG effectively increases the viscosity of aqueous solutions, which may prevent the movement of droplets that causes creaming, even though the droplets were flocculated (Chen et al., 2016).

3.1.3 Creaming index

The emulsions stabilized by WPI alone showed rapid and the highest creaming index (90.63-92.63 %). However, with the addition of 0.25 wt% XG, creaming index of emulsion was significantly reduced (2.11-17.23 %) and no creaming was observed in emulsions in the presence of 0.5 wt% XG (Table 1). This decrease in creaming index in presence of XG might be due to increase in viscosity that prevents the mobility of oil droplets. Velez et al. (2003) reported that the presence of polysaccharides (at ~ > 0.1 wt%) reduced the

298 creaming rate of emulsion. Addition of non-adsorbing biopolymer at certain level increase
299 the continuous phase viscosity which limits the droplets movement resulting a decrease in
300 creaming rate (McClements, 2015). It was observed that emulsion system with the highest
301 viscosity showed the highest emulsion stability and the lowest creaming index (Table 1).
302 However, emulsion viscosity cannot be always linked with emulsion stability. The
303 emulsion stability is further dependent on biopolymer nature and pH of emulsion system
304 (Owens et al., 2018). The stability of emulsion at pH 7 attributes that at this pH both
305 protein and XG carried negative charge, thus anion groups on XG adsorbed to cationic
306 patches on protein molecule, which provide the electrostatic and steric repulsion between
307 droplet surface (Qiu et al., 2015a). Furthermore, XG provided the high viscosity within
308 continuous phase, which limited creaming instability (Xu et al., 2017). In the present study,
309 WPI stabilized emulsion in the presence of 0.5 wt% XG remained stable with no sign of
310 creaming at 25 ºC for one month (Fig. S1, supplementary material).

311

312 Finally, based on higher emulsion viscosity, emulsion stability and lower creaming index
313 (Table 1), the astaxanthin-loaded WPI-XG emulsion systems with varying concentration of
314 WPI (2, 3, 4 and 5 wt%) and fixed concentration of XG (0.5 wt%) were selected for further
315 particle characterization and classified as E1, E2, E3 and E4 respectively.

316 **3.2 Effect of WPI on the particle characteristics of astaxanthin-loaded WPI-XG**
317 **emulsions**

318 The particle characteristics of WPI-XG emulsions (E1– E4) with varying concentrations of
319 WPI (2-5 wt%) and XG (0.5 wt%) were determined (Table 2). The mean particle diameter
320 of each WPI-XG emulsions systems was significantly different (ranging from 1.71 to 2.85
321 µm). Further, it was observed to decrease significantly ($p < 0.05$) with the increase in WPI

concentration. The smallest droplet size was exhibited by WPI-XG emulsions system containing higher (5 wt%) WPI concentration. Similarly, Huck-Iriart et al. (2013) reported a decrease in volume-weighted mean diameter ($D_{4,3}$, 4.47 to 0.41 µm) of emulsions with the increase in sodium caseinate concentration (0.2-5 wt%) in the presence of XG (0.5 wt%).

Polydispersity index (PDI) indicates the width of particle size distribution, which ranges from 0 to 1. The lower PDI value (0.1-0.25) shows a relatively narrow size distribution, while the value of PDI more than 0.5 indicates a highly broad distribution (Tamjidi et al., 2014a). The PDI value of all WPI-XG emulsion systems exceeded 0.25 indicating the broad particle size distribution. However, the E3 emulsion system (4% WPI + 0.5% XG) exhibited significantly lower PDI value (0.26) in comparison to other emulsion systems.

Zeta potential exhibits the nature of the electrostatic potential near the droplet surface. A higher zeta potential indicates the greater electrostatic repulsion and separation distance between droplets resulting in reduced flocculation and aggregation (Thaiphanit et al., 2016). The zeta potential between -10 mV and +10 mV is considered nearly neutral, whereas zeta potential value more than +30 mV or less than -30 mV are indicated strongly cationic and anionic respectively (Dizaj et al., 2016). Study of zeta potential of WPI-XG emulsion (E1-E4) showed that all emulsions systems except E3 exhibited more than -30 mV zeta potential. This indicates relatively high negative charge that generates strong electrostatic repulsion preventing droplets coalescence and flocculation (Jain and Anal, 2018).

The microscopic images obtained by light microscope (Fig. 1) indicated that the flocculation occurred without phase separation in the E3 and E4 WPI-XG emulsion systems, while no flocculation was observed in the WPI-XG emulsion systems E1 and E2.

The microstructure, therefore, indicated that droplet flocculation increased with increase in WPI concentration. This result corroborates with results of zeta potential, such that E3 and E4 emulsion system exhibited lower negative value of zeta potential and hence weak electrostatic repulsion. Since, there was no significant difference in the zeta potential of E1 and E2 emulsion system, only the emulsion system E1was selected for further evaluation of the stability of astaxanthin and *in vitro* digestion behavior.

3.3 Effect of storage temperatures on thermal stability of the astaxanthin-loaded emulsion

The thermal stability of astaxanthin was evaluated by determining the total color difference (ΔE) and astaxanthin concentration during storage of astaxanthin-loaded emulsions at different temperature (5, 25, 37, 55 and 70 °C) for 15 days. The changes in emulsion color stored at different incubation temperature was noted using colorimeter to obtain the CIE *L*a*b** color coordinates throughout the storage period. The lightness of the emulsion gradually increased at lower incubation temperature while there was sharp increase in lightness of emulsion incubated at higher temperature (Fig. 2A). On the other hand, redness and yellowness of the emulsion remained relatively stable at the lowest incubation temperatures (Fig. 2B and 2C respectively) and started to decrease gradually with the increase in incubation time and temperature. Oxidation of astaxanthin causes the reduction in red and yellow color of astaxanthin. In addition, the product of oxidation is colorless compounds, such as epoxides and hydroxyl compound (Niamnuy et al., 2008). Besides the color fading caused by the oxidation, Niamnuy et al. (2008) reported the change of color of dried shrimp (the color belongs to astaxanthin pigment) due to astaxanthin isomerization occurring simultaneously with the oxidation of astaxanthin. Moreover, higher total color difference was observed at in the emulsion stored at elevated temperature (55 and 70 °C) compared to emulsion incubated at lower temperature (5, 25 and 37 °C) indicating that

color degradation is strongly dependent on storage temperature (Fig. 2D). Similar result was reported by Davidov-Pardo et al. (2016) who demonstrated the effect of storage temperature on the rate of color fading in lutein (a xanthophyll class of carotenoids).

Further, the thermal stability of astaxanthin at different storage temperatures was determined in terms of the astaxanthin concentration remaining in emulsion and expressed as astaxanthin retention (%) (Fig. 3). The initial astaxanthin retention (100%) was observed to decrease with the increase in storage time and temperature. The stability of astaxanthin was the highest in emulsion stored at 5 °C with only 9% loss after 15 days of storage. Astaxanthin retention was lower for emulsions stored at high temperature (55 and 70 °C) compared to low temperature (5, 25 and 37 °C). Astaxanthin retention profile followed a similar trend with previous studies which reported faster astaxanthin degradation during storage at elevated temperatures (Davidov-Pardo et al., 2016; Liu et al., 2016; Shrestha et al., 2018). An increase in astaxanthin degradation at high temperatures might be due to the effect of heat causing an acceleration of a collision of astaxanthin-loaded emulsified droplets with pro-oxidant, resulting in the stimulation of rate of oxidation reaction (Tamjidi et al., 2014b).

The degradation of astaxanthin concentration was estimated by following the first-order kinetic reaction as demonstrated by previous studies (Bustamante et al., 2016; (Bustos-garza et al., 2013) (Vakarelova et al., 2017). Table 3 represents the degradation rate constant (day^{-1}) and activation energy of reduction in astaxanthin. The astaxanthin degradation constant rate was found to increase with the increase in storage temperature. There was no significant difference ($p > 0.05$) in the astaxanthin degradation constant rate for 5 °C (0.68 day^{-1}) and 25 °C (0.99 day^{-1}), while it was significantly higher for 37 °C (1.33day^{-1}), 55 °C (4.72 $^{-}day^{1}$) and 70 °C (7.90 day^{-1}). The activation energy was 31.55 KJ mol^{-1} which was higher than the activation energy of color fading.

3.4 *In vitro* digestion of astaxanthin-loaded emulsion

3.4.1 Droplet size

Initially, the mean droplet diameter was 1.53 and 2.89 µm for emulsions stabilized by WPI-only and WPI-XG respectively (Fig. 4A). After incubation in SSF, there was significant ($p < 0.05$) increase in the mean particle diameter of emulsion stabilized by WPI alone (2.24 µm). An increased in droplet size could be due to the presence of mucin and mineral ions in the simulated saliva fluid such that mucin, a charged glycoprotein which can promote bridging and/or depletion flocculation (Qiu et al., 2015a), and mineral ions can impact on surface electrostatic effects (Qiu et al., 2015b). Conversely, there were no significant changes in the mean particle diameter of WPI-XG stabilized emulsion. This indicated that the addition of XG could prevent droplet flocculation in the mouth phase.

The particle size of both emulsion systems was significantly increased after passing through the simulated gastric conditions. An increased in the mean droplet diameter could be due to various physicochemical mechanisms including (i) the highly ionic strength within gastric fluid decreased the electrostatic repulsion between droplets surfaced, (ii) hydrolysis of protein by pepsin could decrease the stability of droplet from aggregation (Golding et al., 2011), (iii) some of protein-coated droplets might be replaced by other surface molecules present in the system (Qiu et al., 2015a).

After incubation in SIF, the increase in droplet diameter was observed for both emulsion systems. This increase in droplet size might be due to droplet aggregation and coalescence, caused by the digestion of oil phase and displacement of lipid digestion products such as free fatty acids, monoacylglycerols and diacylglycerols due to the action of pancreatin (Xu et al., 2014). On the other hand, the mean droplet size of emulsion stabilized by WPI-alone (6.67 µm) was significantly ($p< 0.05$) larger than emulsion stabilized by WPI-XG (5.26

420 µm). The small droplet size in emulsion with WPI-XG might be attributed to the presence
421 of XG, that can potentially prevent the formation of the large particles after digestion (Qiu
422 et al., 2015a).

423 3.4.2 Zeta potential

424 Zeta potential exhibits the electrical characteristic of emulsified droplets and indicates the
425 changes in the interfacial composition of the emulsion after passing through each stage of
426 digestion. At initial stage zeta potential of WPI and WPI-XG stabilized emulsion was -32.8
427 and -34.9 mV respectively (Fig. 4B). After passing through simulated mouth conditions,
428 both emulsion system exhibited anionic zeta potential indicating no variation on interfacial
429 composition in consistent with the droplet size. As emulsions were incubated in SGF, the
430 magnitude of zeta potential of both emulsions changed appreciably to positive charge. This
431 change in zeta potential might be due to pH of SGF being lower than the isoelectric point
432 of WPI (pI = 4.5), which in turn reduced anionic charge of XG by increasing cationic
433 charge of WPI, or may be due to replacement of original emulsifier by the action of pepsin
434 digested WPI (Shrestha et al., 2018).

435 Finally, on passing from gastric to small intestinal phase, the zeta potential was -10.0 mV
436 for WPI emulsion and -24.9 mV for WPI-XG stabilized emulsion. The decline in zeta
437 potential might be due to the fact that some of WPI coated droplets were digested by
438 pepsin or displaced by lipid digestion products. However, the emulsion stabilized by WPI-
439 XG exhibited significantly higher negative charge indicating the presence of XG on coated
440 droplets (Xu et al., 2014).

441 3.4.3 Free fatty acid released

442 The rate of free fatty acids released was significantly different ($p<0.05$) by the emulsion
443 systems stabilized by WPI-alone and WPI-XG (Fig. 4C). There was initially a rapid release

444 of free fatty acids from both emulsion systems during the first 20 min, followed by an
445 almost constant release of free fatty acids along with the digestion time. However, the rate
446 of free fatty acids released was higher in emulsion stabilized by WPI alone compared to
447 WPI-XG stabilized emulsion during the first 20 min of digestion till at the end of digestion
448 time (120 min). This indicated that the presence of XG impacts on the fat digestion.
449 Similarly, Espert et al. (2019) found a reduction (68%) in the amount of free fatty acids
450 released from cream containing XG as comparison to cream without XG. The
451 incorporation of XG may inhibit the lipid digestion by restricting the access of bile salt and
452 lipase to react efficiently at the lipid droplet surface.
453
454 3.4.4 Digestion of astaxanthin

455 Finally, the influence of emulsion stabilized by WPI-alone and WPI-XG emulsion system
456 on the solubilization of astaxanthin in the micelle phase was examined (Fig. 5). After the
457 final stage of *in vitro* digestion, the digesta was collected and centrifuged. Three layers
458 were developed after centrifugation, including the bottom sediment phase, the middle
459 micelle phase, and the upper oil phase. The middle phase was yellowish-orange and
460 optically transparent which suggested that astaxanthin was solubilized in small mixed
461 micelles. The extent of released astaxanthin was 46.2% and 12.6% from emulsion with
462 WPI alone and WPI-XG stabilized emulsion. A similar result was reported by Xu et al.
463 (2014) who reported 45.5% and 23.0% of β-carotene was observed to be released from
464 emulsion stabilized by WPI and the mixture of WPI-beet pectin, respectively, into water-
465 soluble mixed micelles.

466 There was consistency between the extent of free fatty acid formation and the amount of
467 astaxanthin released. The lower astaxanthin release from emulsion containing XG might be
468 due to the fact that presence of XG limited the access of bile salt and lipase to react at lipid

droplet surface, thus inhibited the formation of micelles and astaxanthin still remained in non-digested droplets, as a consequent decreased the solubility of astaxanthin into the aqueous phase (Zhang et al., 2015), secondly the binding of XG to the released astaxanthin might result in the formation of a dense molecular complex (Yonekura and Nagao, 2007; Mun et al., 2016).

4. Conclusion

Astaxanthin-loaded oil-in-water emulsion was stabilized by WPI and XG. The addition of XG significantly increased emulsion stability in comparison to emulsions stabilized by WPI alone. No creaming was observed in the WPI-XG emulsions containing 0.5 wt% XG. The astaxanthin encapsulated WPI-XG emulsion system was more stable at low temperature of storage (5, 25 and 37 ºC). During *in vitro* digestion, emulsion stabilized by WPI-XG exhibited the smaller droplet size within gastric and intestinal phase indicating the addition of XG can improve the stability of protein-stabilized emulsion. The presence of XG in combination with WPI demonstrated lower lipid digestibility and limited the content of released free fatty acid. Further, the combination of WPI-XG reduced the digestion and released of astaxanthin in comparison to emulsion system stabilized by WPI alone. This study signifies the application of economical and easily accessible biopolymers, i.e. WPI and XG in the formulation of astaxanthin enriched stable emulsions for food and feed applications. The provided results are useful for designing functional foods (such as mayonnaise, sauce, gravy, and salad dressing) fortified with health-promoting ingredient.

Conflict of interest:

The authors declare no conflict of interest.

Funding:

This research did not receive any specific grant from funding agencies in the public, commercial, or not-for-profit sectors

References

Anal, A.K., Shrestha, S., Sadiq, M.B., 2019. Biopolymeric-based emulsions and their effects during processing, digestibility and bioaccessibility of bioactive compounds in food systems. Food Hydrocolloids 87, 691–702. https://doi.org/10.1016/j.foodhyd.2018.09.008

Bouyer, E., Mekhloufi, G., Huang, N., Rosilio, V., Agnely, F., 2013. β-Lactoglobulin, gum arabic, and xanthan gum for emulsifying sweet almond oil: Formulation and stabilization mechanisms of pharmaceutical emulsions. Colloids and Surfaces A: Physicochemical and Engineering Aspects 433, 77–87. https://doi.org/10.1016/j.colsurfa.2013.04.065

Bouyer, E., Mekhloufi, G., Rosilio, V., Grossiord, J.L., Agnely, F., 2012. Proteins, polysaccharides, and their complexes used as stabilizers for emulsions: Alternatives to synthetic surfactants in the pharmaceutical field? International Journal of Pharmaceutics 436, 359–378. https://doi.org/10.1016/j.ijpharm.2012.06.052

Bustamante, A., Masson, L., Velasco, J., Del Valle, J.M., Robert, P., 2016. Microencapsulation of H. pluvialis oleoresins with different fatty acid composition: Kinetic stability of astaxanthin and alpha-tocopherol. Food Chemistry 190, 1013–1021. https://doi.org/10.1016/j.foodchem.2015.06.062

515 Bustos-garza, C., Yáñez-fernández, J., Barragán-huerta, B.E., 2013. Thermal and pH
516 stability of spray-dried encapsulated astaxanthin oleoresin from Haematococcus
517 pluvialis using several encapsulation wall materials. Food Research International 54,
518 641–649. https://doi.org/10.1016/j.foodres.2013.07.061

519 Calvano, C.D., Zambonin, C.G., Foti, C., Cassano, N., Vena, G.A., 2008. A matrix assisted
520 laser desorption ionization time-of-flight mass spectrometry investigation to assess
521 the composition of cod liver oil based products which displayed a different in vivo
522 allergenic power. Food and Chemical Toxicology 46, 3580–3585.
523 https://doi.org/10.1016/j.fct.2008.08.036

524 Chen, X., Li, W., Zhao, Q., Selomulya, C., Zhu, X., Xiong, H., 2016. Physical and
525 Oxidative Stabilities of O/W Emulsions Formed with Rice Dreg Protein Hydrolysate:
526 Effect of Xanthan Gum Rheology. Food and Bioprocess Technology 9, 1380–1390.
527 https://doi.org/10.1007/s11947-016-1727-9

528 Chityala, P.K., Khouryieh, H., Williams, K., Conte, E., 2016. Effect of xanthan/enzyme-
529 modified guar gum mixtures on the stability of whey protein isolate stabilized fish oil-
530 in-water emulsions. Food Chemistry 212, 332–340.
531 https://doi.org/10.1016/J.FOODCHEM.2016.05.187

532 Davidov-Pardo, G., Gumus, C.E., McClements, D.J., 2016. Lutein-enriched emulsion-
533 based delivery systems: Influence of pH and temperature on physical and chemical
534 stability. Food Chemistry 196, 821–827.
535 https://doi.org/10.1016/j.foodchem.2015.10.018

536 Dizaj, S.M., Yaqoubi, S., Adibkia, K., Lotfipour, F., 2016. 9 - Nanoemulsion-based
537 delivery systems: preparation and application in the food industry, Emulsions. Editor:
538 Alexandru Mihai Grumezescu. Elsevier Inc.

https://doi.org/http://dx.doi.org/10.1016/B978-0-12-804306-6.00009-X

Donald, A.M., 2008. Aggregation in β-lactoglobulin. Soft Matter 4, 1147–1150. https://doi.org/10.1039/b800106e

Espert, M., Constantinescu, L., Sanz, T., Salvador, A., 2019. Effect of xanthan gum on palm oil in vitro digestion. Application in starch-based filling creams. Food Hydrocolloids 86, 87–94. https://doi.org/10.1016/j.foodhyd.2018.02.017

Farvin, K. S., Andersen, L. L., Nielsen, H. H., Jacobsen, C., Jakobsen, G., Johansson, I., & Jessen, F., 2014. Antioxidant activity of Cod (*Gadus morhua*) protein hydrolysates: In vitro assays and evaluation in 5% fish oil-in-water emulsion. Food chemistry, 149, 326-334.

Feng, Z.Z., Li, M.Y., Wang, Y.T., Zhu, M.J., 2018. Astaxanthin from Phaffia rhodozyma: Microencapsulation with carboxymethyl cellulose sodium and microcrystalline cellulose and effects of microencapsulated astaxanthin on yogurt properties. LWT - Food Science and Technology 96, 152–160. https://doi.org/10.1016/j.lwt.2018.04.084

Golding, M., Wooster, T.J., Day, L., Xu, M., Lundin, L., Keogh, J., Cliftonx, P., 2011. Impact of gastric structuring on the lipolysis of emulsified lipids. Soft Matter. https://doi.org/10.1039/c0sm01227k

Guzey, D., McClements, D.J., 2006. Formation, stability and properties of multilayer emulsions for application in the food industry. Advances in Colloid and Interface Science 128–130, 227–248. https://doi.org/10.1016/J.CIS.2006.11.021

Huck-Iriart, C., Pizones Ruiz-Henestrosa, V.M., Candal, R.J., Herrera, M.L., 2013. Effect of Aqueous Phase Composition on Stability of Sodium Caseinate/Sunflower oil Emulsions. Food and Bioprocess Technology 6, 2406–2418.

https://doi.org/10.1007/s11947-012-0901-y

Jain, S., Anal, A.K., 2018. Preparation of eggshell membrane protein hydrolysates and culled banana resistant starch-based emulsions and evaluation of their stability and behavior in simulated gastrointestinal fluids. Food Research International 103, 234–242. https://doi.org/10.1016/j.foodres.2017.10.042

Khalid, N., Shu, G., Holland, B.J., Kobayashi, I., Nakajima, M., Barrow, C.J., 2017. Formulation and characterization of O/W nanoemulsions encapsulating high concentration of astaxanthin. Food Research International. https://doi.org/10.1016/j.foodres.2017.06.019

Khouryieh, H., Puli, G., Williams, K., Aramouni, F., 2015. Effects of xanthan–locust bean gum mixtures on the physicochemical properties and oxidative stability of whey protein stabilised oil-in-water emulsions. Food Chemistry 167, 340–348. https://doi.org/10.1016/J.FOODCHEM.2014.07.009

Liu, X., McClements, D.J., Cao, Y., Xiao, H., 2016. Chemical and Physical Stability of Astaxanthin-Enriched Emulsion-Based Delivery Systems. Food Biophysics 11, 302–310. https://doi.org/10.1007/s11483-016-9443-6

Martínez-Delgado, A.A., Khandual, S., Villanueva–Rodríguez, S.J., 2017. Chemical stability of astaxanthin integrated into a food matrix: Effects of food processing and methods for preservation. Food Chemistry 225, 23–30. https://doi.org/10.1016/j.foodchem.2016.11.092

McClements, D.J., 2015. Emulsion formation, in: Food Emulsions Principles, Practices, and Techniques. Third edition ed CRC Press, Boca Raton, FL. https://doi.org/10.1093/acprof:oso/9780195383607.003.0002

585 Meor Mohd Affandi, M.M.R., Julianto, T., Majeed, A.B.A., 2011. Development and
586 stability evaluation of Astaxanthin nanoemulsion. Asian Journal of Pharmaceutical
587 and Clinical Research 4, 143–148.

588 Moschakis, T., Murray, B.S., Dickinson, E., 2005. Microstructural evolution of
589 viscoelastic emulsions stabilised by sodium caseinate and xanthan gum. Journal of
590 Colloid and Interface Science 284, 714–728.
591 https://doi.org/10.1016/j.jcis.2004.10.036

592 Mun, S., Park, S., Kim, Y.R., McClements, D.J., 2016. Influence of methylcellulose on
593 attributes of β-carotene fortified starch-based filled hydrogels: Optical, rheological,
594 structural, digestibility, and bioaccessibility properties. Food Research International
595 87, 18–24. https://doi.org/10.1016/j.foodres.2016.06.008

596 Niamnuy, C., Devahastin, S., Soponronnarit, S., Vijaya Raghavan, G.S., 2008. Kinetics of
597 astaxanthin degradation and color changes of dried shrimp during storage. Journal of
598 Food Engineering 87, 591–600. https://doi.org/10.1016/j.jfoodeng.2008.01.013

599 Owens, C., Griffin, K., Khouryieh, H., Williams, K., 2018. Creaming and oxidative
600 stability of fish oil-in-water emulsions stabilized by whey protein-xanthan-locust bean
601 complexes: Impact of pH. Food Chemistry 239, 314–322.
602 https://doi.org/10.1016/J.FOODCHEM.2017.06.096

603 Ozturk, B., McClements, D.J., 2016. Progress in natural emulsifiers for utilization in food
604 emulsions. Current Opinion in Food Science 7, 1–6.
605 https://doi.org/10.1016/j.cofs.2015.07.008

606 Park, S., Mun, S., Kim, Y.R., 2018. Effect of xanthan gum on lipid digestion and
607 bioaccessibility of β-carotene-loaded rice starch-based filled hydrogels. Food

608 Research International 105, 440–445. https://doi.org/10.1016/j.foodres.2017.11.039

609 Pinsirodom, P., Parkin, K.L., 2001. Lipase Assays. Current Protocols in Food Analytical
610 Chemistry 00, C3.1.1-C3.1.13. https://doi.org/10.1002/0471142913.fac0301s00

611 Protonotariou, S., Evageliou, V., Yanniotis, S., Mandala, I., 2013. The influence of
612 different stabilizers and salt addition on the stability of model emulsions containing
613 olive or sesame oil. Journal of Food Engineering 117, 124–132.
614 https://doi.org/10.1016/j.jfoodeng.2013.01.044

615 Qiu, C., Zhao, M., Decker, E.A., McClements, D.J., 2015a. Influence of anionic dietary
616 fibers (xanthan gum and pectin) on oxidative stability and lipid digestibility of wheat
617 protein-stabilized fish oil-in-water emulsion. Food Research International 74, 131–
618 139. https://doi.org/10.1016/j.foodres.2015.04.022

619 Qiu, C., Zhao, M., Decker, E.A., McClements, D.J., 2015b. Influence of protein type on
620 oxidation and digestibility of fish oil-in-water emulsions: Gliadin, caseinate, and
621 whey protein. Food Chemistry 175, 249–257.
622 https://doi.org/10.1016/j.foodchem.2014.11.112

623 Ribeiro, H.S., Rico, L.G., Badolato, G.G., Schubert, H., 2005. Production of O/W
624 Emulsions Containing Astaxanthin by Repeated Premix Membrane Emulsification.
625 Journal of Food Science 70, E117–E123. https://doi.org/10.1111/j.1365-
626 2621.2005.tb07083.x

627 Salvia-Trujillo, L., Qian, C., Martín-Belloso, O., McClements, D.J., 2013. Influence of
628 particle size on lipid digestion and beta-carotene bioaccessibility in emulsions and
629 nanoemulsions. Food Chemistry 141, 1475–1480.
630 https://doi.org/10.1016/j.foodchem.2013.03.050

631 Shrestha, S., Sadiq, M.B., Anal, A.K., 2018. Culled banana resistant starch-soy protein
632 isolate conjugate based emulsion enriched with astaxanthin to enhance its stability.
633 International Journal of Biological Macromolecules 120.
634 https://doi.org/10.1016/j.ijbiomac.2018.08.066

635 Sun, C., Gunasekaran, S., Richards, M.P., 2007. Effect of xanthan gum on
636 physicochemical properties of whey protein isolate stabilized oil-in-water emulsions.
637 Food Hydrocolloids. https://doi.org/10.1016/j.foodhyd.2006.06.003

638 Taksima, T., Limpawattana, M., Klaypradit, W., 2015. Astaxanthin encapsulated in beads
639 using ultrasonic atomizer andapplication in yogurt as evaluated by consumer sensory
640 profile. LWT - Food Science and Technology 62, 431–437.
641 https://doi.org/10.1016/j.lwt.2015.01.011

642 Tamjidi, F., Shahedi, M., Varshosaz, J., Nasirpour, A., 2014a. Design and characterization
643 of astaxanthin-loaded nanostructured lipid carriers. Innovative Food Science and
644 Emerging Technologies 26, 366–374. https://doi.org/10.1016/j.ifset.2014.06.012

645 Tamjidi, F., Shahedi, M., Varshosaz, J., Nasirpour, A., 2014b. EDTA and α-tocopherol
646 improve the chemical stability of astaxanthin loaded into nanostructured lipid carriers.
647 European Journal of Lipid Science and Technology 116, 968–977.
648 https://doi.org/10.1002/ejlt.201300509

649 Tamnak, S., Mirhosseini, H., Tan, C.P., Ghazali, H.M., Muhammad, K., 2016.
650 Physicochemical properties, rheological behavior and morphology of pectin-pea
651 protein isolate mixtures and conjugates in aqueous system and oil in water emulsion.
652 Food Hydrocolloids 56, 405–416. https://doi.org/10.1016/j.foodhyd.2015.12.033

653 Thaiphanit, S., Schleining, G., Anprung, P., 2016. Food Hydrocolloids Effects of coconut (

654 Cocos nucifera L .) protein hydrolysates obtained from enzymatic hydrolysis on the
655 stability and rheological properties of oil-in-water emulsions. Food hydrocolloids 60,
656 252–264. https://doi.org/10.1016/j.foodhyd.2016.03.035

657 Vakarelova, M., Zanoni, F., Lardo, P., Rossin, G., Mainente, F., Chignola, R., Menin, A.,
658 Rizzi, C., Zoccatelli, G., 2017. Production of stable food-grade microencapsulated
659 astaxanthin by vibrating nozzle technology. Food Chemistry 221, 289–295.
660 https://doi.org/10.1016/j.foodchem.2016.10.085

661 Velez, G., Fernandez, M.A., Munoz, J., Williams, P.A., English, R.J., 2003. Role of
662 hydrocolloids in the creaming of oil in water emulsions. Journal of agricultural and
663 food chemistry 51, 265–269. https://doi.org/10.1021/jf020664n

664 Xu, D., Yuan, F., Gao, Y., Panya, A., McClements, D.J., Decker, E.A., 2014. Influence of
665 whey protein-beet pectin conjugate on the properties and digestibility of β-carotene
666 emulsion during in vitro digestion. Food Chemistry.
667 https://doi.org/10.1016/j.foodchem.2014.02.019

668 Xu, X., Luo, L., Liu, C., McClements, D.J., 2017. Utilization of anionic polysaccharides to
669 improve the stability of rice glutelin emulsions: Impact of polysaccharide type, pH,
670 salt, and temperature. Food Hydrocolloids 64, 112–122.
671 https://doi.org/10.1016/j.foodhyd.2016.11.005

672 Yonekura, L., Nagao, A., 2007. Intestinal absorption of dietary carotenoids. Molecular
673 Nutrition and Food Research 51, 107–115. https://doi.org/10.1002/mnfr.200600145

674 Zhang, C., Xu, W., Jin, W., Shah, B.R., Li, Y., Li, B., 2015. Influence of anionic alginate
675 and cationic chitosan on physicochemical stability and carotenoids bioaccessibility of
676 soy protein isolate-stabilized emulsions. Food Research International 77, 419–425.

https://doi.org/10.1016/j.foodres.2015.09.020

680 **Figure Captions**

681 **Fig. 1**. Microscopic images of astaxanthin-loaded emulsions containing 0.5 wt% XG with
682 different WPI concentration (magnification 40×); (E1) 2 wt% WPI + 0.5 wt% XG; (E2) 3
683 wt% WPI + 0.5 wt% XG; (E3) 4 wt% WPI + 0.5 wt% XG; (E4) 5 wt% WPI + 0.5 wt%
684 XG

685 **Fig. 2**. Effect of the storage temperature on the lightness (*L**) (A); redness (*a**) (B);
686 yellowness (*b**) (C); total color (ΔE) (D) of the astaxanthin-loaded emulsion incubated at
687 different temperatures.

688 **Fig. 3**. Effect of storage temperature on astaxanthin retention of the astaxanthin-loaded
689 emulsion incubated at different temperatures.

690 **Fig. 4**. Changes in droplet properties: the mean particle diameter (A); zeta-potential (B)
691 throughout the *in vitro* digestion model; and free fatty acids (FFA %) released in the
692 intestine phase (C) of the emulsions stabilized by WPI and WPI-XG. Different capital
693 letters (A-C) indicate significant differences ($p < 0.05$) in the mean particle size (z-
694 average) when samples were compared between different stages of *in vitro* digestion (same
695 emulsion system). Different lowercase letters (a-b) indicate significant differences ($p <$
696 0.05) between emulsion systems (within same *in vitro* digestion stage).

697 **Fig. 5.** Effect of WPI and WPI-XG stabilized emulsions on the digestion of astaxanthin.
698 Different lowercase letters (a, b) indicate significant differences ($p < 0.05$) in the
699 astaxanthin digestion between emulsion systems (WPI and WPI-XG stabilized emulsion).

700 **Table 1** Effect of WPI and XG on emulsion viscosity, stability and creaming index of
701 WPI-XG stabilized emulsion

Composition (% wt)			Viscosity	Emulsion stability	Creaming index
WPI	XG	Oil	(mPa.s)	(%)	(%)
2	0	13.0	5.55 ± 0.24^{g}	7.22 ± 1.74^{e}	91.58 ± 0.42^{a}
	0.25	12.75	186.13 ± 0.78^{e}	94.97 ± 0.32^{bc}	17.23 ± 0.47^{b}
	0.5	12.5	582.2 ± 0.72^{b}	99.02 ± 0.35^{a}	0.00 ± 0.0^{e}
3	0	12.0	5.80 ± 0.23^{g}	6.11 ± 0.48^{e}	90.63 ± 0.76^{a}
	0.25	11.75	186.03 ± 1.53^{e}	92.87 ± 2.29^{cd}	5.61 ± 1.61^{c}
	0.5	11.5	583.1 ± 0.50^{b}	96.86 ± 1.00^{ab}	0.00 ± 0.0^{e}
4	0	11.0	6.97 ± 0.12^{g}	5.83 ± 0.84^{e}	92.14 ± 0.32^{a}
	0.25	11.75	192.93 ± 1.75^{d}	95.13 ± 1.64^{bc}	4.38 ± 0.80^{c}
	0.5	11.5	584.0 ± 0.92^{ab}	97.19 ± 0.51^{ab}	0.00 ± 0.0^{e}
5	0	10.0	12.22 ± 0.49^{f}	6.67 ± 0.84^{e}	92.63 ± 0.53^{a}
	0.25	9.75	218.40 ± 0.82^{c}	89.61 ± 1.3^{d}	2.11 ± 1.06^{d}
	0.5	9.5	586.4 ± 0.53^{a}	94.39 ± 1.73^{bc}	0.00 ± 0.0^{e}

702 Different superscript letters (a-g) indicate significant differences ($p < 0.05$) within the
703 column

704

705

706

707

708 **Table 2** Particle size, polydispersity index (PDI) and zeta potential of astaxanthin-loaded
709 emulsions containing 0.5 wt% XG at different WPI concentration

Emulsion systems	Composition (wt%)	Mean particle diameter (μm)	Polydispersity index	Zeta potential (mV)
E1	2% WPI + 0.5% XG	2.85 ± 0.12^{a}	0.33 ± 0.04^{ab}	-34.9 ± 1.31^{a}
E2	3% WPI + 0.5% XG	2.53 ± 0.16^{b}	0.43 ± 0.04^{a}	-36.2 ± 0.29^{a}
E3	4% WPI + 0.5% XG	2.09 ± 0.07^{c}	0.26 ± 0.06^{b}	-28.2 ± 0.34^{c}
E4	5% WPI + 0.5% XG	1.71 ± 0.07^{d}	0.43 ± 0.14^{a}	-30.6 ± 0.59^{b}

710 Different superscript letters (a-d) indicate the significant differences ($p < 0.05$) in the same
711 column.

712

713 **Table 3** Astaxanthin degradation rate constant of emulsions at different storage

714 temperatures

Storage temperature (°C)	First-order degradation	k $\times 10^{-2}$ (day^{-1})	R^2	Activation energy (kJ/mol)
5	C = 0.456 [-exp (0.0068) t]	0.68^{a}	0.91	31.55
25	C = 0.456 [-exp (0.0099) t]	0.99^{a}	0.90	
37	C = 0.456 [-exp (0.0133) t]	1.33^{b}	0.93	
55	C = 0.456 [-exp (0.0472) t]	4.72^{c}	0.97	
70	C = 0.456 [-exp (0.079) t]	7.90^{d}	0.98	

715 C is Concentration of astaxanthin (mg/mL), k is degradation rate constant, R^2 is square of

716 correlation coefficient. Different superscript letters (a-d) indicate the significant ($p < 0.05$)

717 differences among degradation rate constant (k).

718

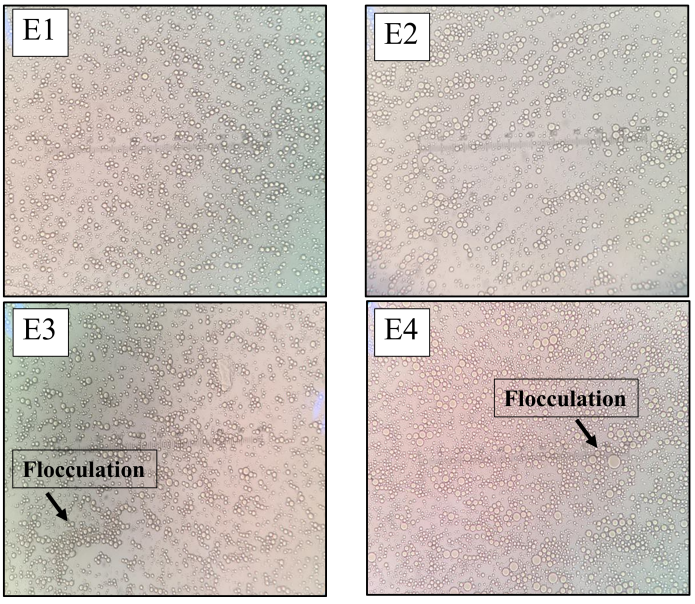

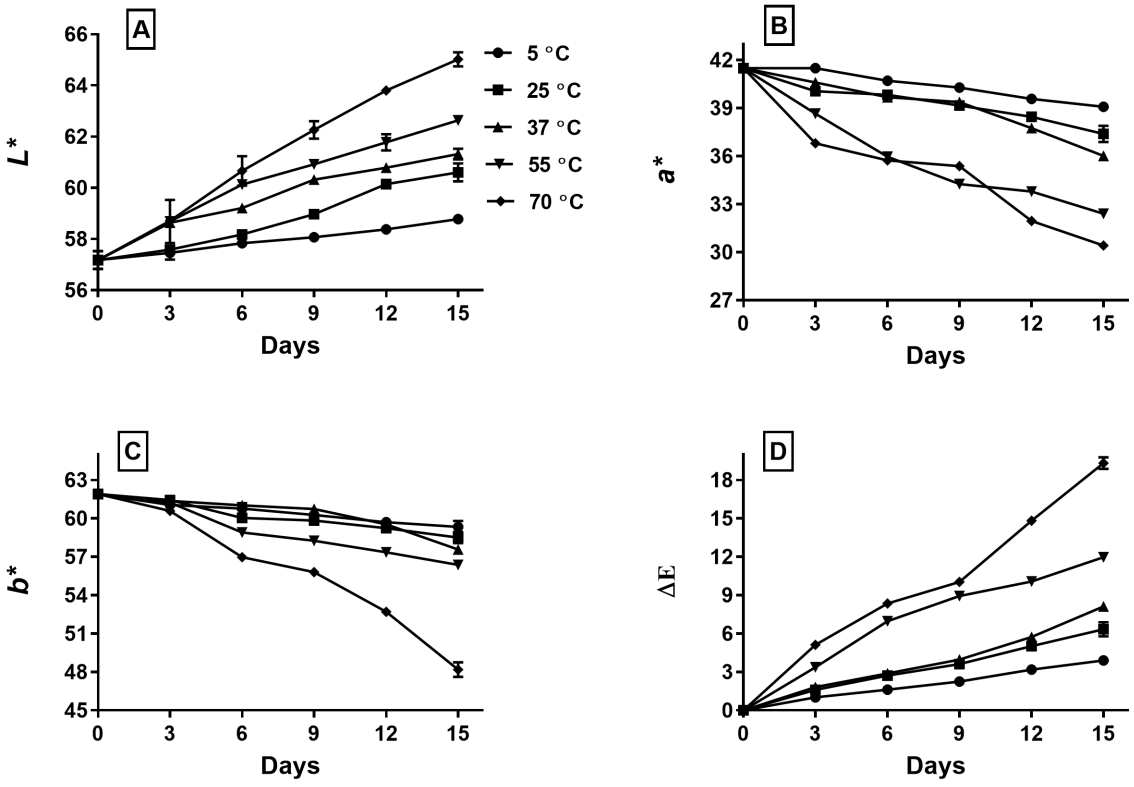
A
L*
66
64
62
60
58
56
0
3
6
9
12
15
Days
5 °C
25 °C
37 °C
55 °C
70 °C
B
a*
42
39
36
33
30
27
0
3
6
9
12
15
Days
C
b*
63
60
57
54
51
48
45
0
3
6
9
12
15
Days
D
ΔE
18
15
12
9
6
3
0
0
3
6
9
12
15
Days

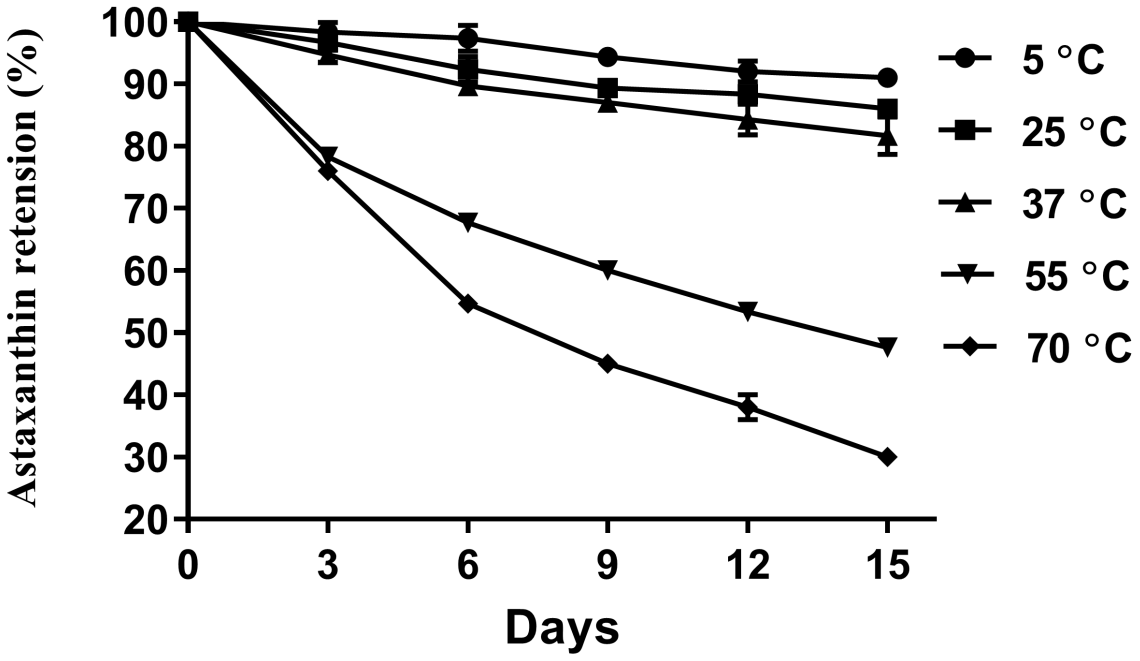

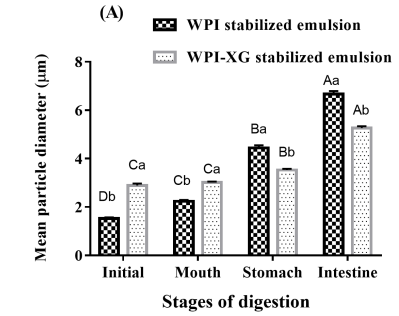
(A)
WPI stabilized emulsion
WPI-XG stabilized emulsion
Mean particle diameter (μm)
8
6
4
2
0
Db
Ca
Cb
Ca
Ba
Bb
Aa
Ab
Initial
Mouth
Stomach
Intestine
Stages of digestion

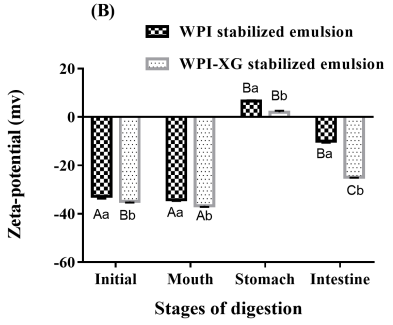
(B)
WPI stabilized emulsion
WPI-XG stabilized emulsion
Zeta-potential (mv)
20
0
-20
-40
-60
Aa
Bb
Aa
Ab
Ba
Bb
Ba
Cb
Initial
Mouth
Stomach
Intestine
Stages of digestion

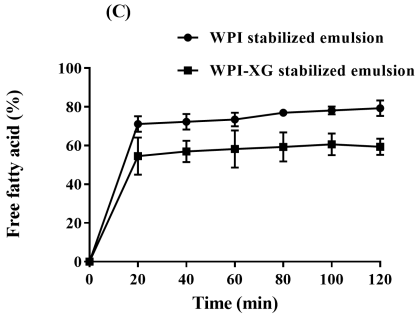
(C)
WPI stabilized emulsion
WPI-XG stabilized emulsion
Free fatty acid (%)
100
80
60
40
20
0
0
20
40
60
80
100
120
Time (min)

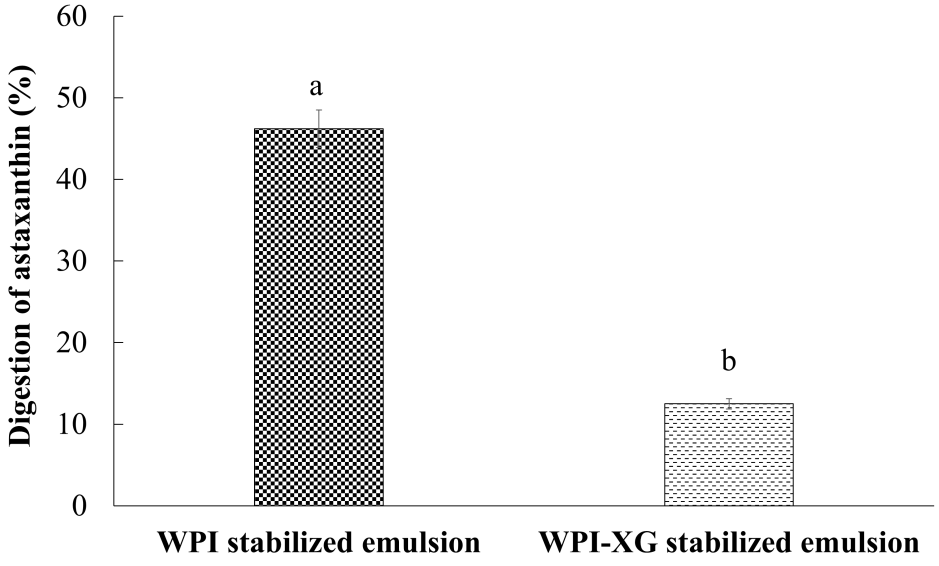
60
50
40
30
20
10
0
Digestion of astaxanthin (%)
a
b
WPI stabilized emulsion
WPI-XG stabilized emulsion

Highlights

- Oil-in-water emulsions with whey protein isolate (WPI) as wall material and xanthan gum (XG, 0.5%) showed better stability
- WPI-XG stabilized emulsions showed higher stability of astaxanthin at lower storage temperature (5-37 °C) for 15 days
- *In vitro* digestibility of astaxanthin was lower in WPI-XG emulsion system as compared to WPI emulsion system (control)